Feature Article

Electrocatalysis via Direct Electrochemistry of Myoglobin Immobilized on Colloidal Gold Nanoparticles

Songqin Liu, Huangxian Ju*

Department of Chemistry, Institute of Analytical Science, State Key Laboratory of Coordination Chemistry, Nanjing University, Nanjing 210093, P. R. China
*e-mail: hxju@nju.edu.cn.

Received: August 12, 2002
Final version: October 14, 2002

Abstract
The direct electron transfer between immobilized myoglobin (Mb) and colloidal gold modified carbon paste electrode was studied. The Mb immobilized on the colloidal gold nanoparticles displayed a pair of redox peaks in 0.1 M pH 7.0 PBS with a formal potential of –(0.108 ± 0.002) V (vs. NHE). The response showed a surface-controlled electrode process with an electron transfer rate constant of (26.7 ± 3.7) s^{-1} at scan rates from 10 to 100 mV s^{-1} and a diffusion-controlled process involving the diffusion of proton at scan rates more than 100 mV s^{-1}. The immobilized Mb maintained its activity and could electrocatalyze the reduction of both hydrogen peroxide and nitrite. Thus, the novel renewable reagentless sensors for hydrogen peroxide and nitrite were developed, respectively. The activity of Mb with respect to the pseudo peroxidase with a K_M^{app} value of 0.65 mM could respond linearly to hydrogen peroxide concentration from 4.6 to 28 μM. The sensor exhibited a fast amperometric response to NO_2^- reduction and reached 93% of steady-state current within 5 s. The linear range for NO_2^- determination was from 8.0 to 112 μM with a detection limit of 0.7 μM at 3σ.

Keywords: Biosensors, Carbon paste electrode, Myoglobin, Direct electron transfer, Electrocatalysis, Colloidal gold

1. Introduction

Myoglobin (Mb) is a small heme protein found in muscle cells. The physiological function of Mb is to store dioxygen and also to increase the diffusion rate of dioxygen in the cell. Although Mb does not function physiologically as an electron carrier, it undergoes the oxidation and reduction process in respiratory system. Thus, its electron transfer reactions play essential roles in biological process. The electrochemistry of Mb has been described in a number of publications such as early on dropping mercury electrodes [1, 2] and later by using methyl viologen modified gold electrode [3, 4] and indium oxide electrode [5]. However, electron transfer between Mb and bare solid electrodes is usually slow and the protein is irreversibly denatured [3]. Great efforts have been made to facilitate electron transfer for Mb by using different mediators or promoters [6, 7]. Among these, the surfactant film technique with which the incorporated Mb can reside in a bilayer, biomembrane-like microenvironment and improve their electrochemical properties is a main method [8–16]. However, the Mb-surfactant films were subject to mechanical damage in stirred electrolytic reactors [17]. Thus, it is necessary to search for a way to develop a new Mb modified electrode with well-behaved electrochemistry and good stability.

It has long been recognized that carbon paste electrodes are very attractive due to their convenient modification by mixing a modifier with the paste [18–21]. The modifier can be in intimate contact and locate in the vicinity of carbon sensing sites, which enhance the electron transfer rate [21, 22]. Colloidal gold, a biocompatible material, has been used for study of the direct electrochemistry of proteins [23, 24]. It provides an environment similar to that of redox proteins in native systems and gives the protein molecules more freedom in orientation, thus reducing the insulating property of the protein shell for the direct electron transfer and facilitating the electron transfer through the conducting tunnels of colloidal gold. Our previous works indicated both cytochrome c and horseradish peroxidase immobilized on colloidal gold modified carbon paste electrode were of good-term stability and high sensitivity [24, 25]. This work studies the electron transfer of Mb by incorporating it into the blend of colloidal gold and carbon paste, in which the colloidal gold is used to retain the bioactivity of Mb and facilitate the direct electron transfer between Mb and carbon sensing sites. The immobilized Mb exhibits a fast electron transfer rate, an electrocatalytic behavior with respect to the pseudo peroxidase activity to hydrogen peroxide reduction and a fast amperometric response to $NaNO_2$.

Both nitrite and hydrogen peroxide exist widely in the environment, beverages, and food products [26, 27]. Therefore, the importance of improved analytical methods for nitrite [28–30] and hydrogen peroxide [31–33] detections in food, water and biological fluids has received considerable attention. This work provides a novel method for preparation of renewable reagentless sensors for both hydrogen peroxide and nitrite.

  DOI: 10.1002/elan.200302722

2. Experimental

2.1. Materials

Horse heart myoglobin (No. M-1882, type III) was purchased from Sigma and used as received. $AuCl_3HCl \cdot 4H_2O$ (Au% > 48%) was obtained from Aldrich. Carbon graphite powder (< 325 mesh, Johnson Matthey) and paraffin oil (from Fluka) were used for the preparation of carbon paste. All other chemicals were of analytical grade and used without further purification. Colloidal gold was prepared as the literature [24]. 0.1 M phosphate buffer solutions (PBS) with various pH values were prepared by mixing stock standard solutions of K_2HPO_4 and KH_2PO_4 and adjusting the pH with 0.1 M H_3PO_4 or NaOH. All solutions were made up with twice-distilled water.

2.2. Electrode Preparation

The carbon paste (CP) was prepared by thoroughly mixing carbon graphite powder pretreated at 700 °C for 30 s and paraffin oil (1 mg : 0.36 μL). The colloidal gold modified carbon paste (Au-CP) was prepared according to the following procedure. 10 mg of pretreated graphite powder was mixed thoroughly with 30 μL 24-nm colloidal gold solution. After evaporation of water in a desiccator for three hours, 3.6 μL paraffin oil was added to the mixture. The Mb-Au-CP was prepared by adding 3.6 μL paraffin oil and 3.0 mg Mb to the dried mixture of 30 μL colloidal gold solution and 10 mg carbon graphite powder. As a comparison, 3.0 mg Mb, 10 mg carbon graphite powder were mixed thoroughly with 3.6 μL paraffin oil for preparation of Mb-CP. A portion of the resulting pastes was put into plastic syringe tubes with the inner diameter of 0.51 ± 0.01 mm to form different electrodes (CPE, Au-CPE, Mb-Au-CPE and Mb-CPE). Electrical contact to the pastes was established by inserting a copper wire down the plastic syringe tube and into the back of the mixture. The resulted electrodes were stored at 4 °C. After the electrode tips were smoothed manually with clean paper and then at a plane glass surface to produce the flat surface, following experiments were carried out.

2.3. Electrochemical Measurements

Electrochemical measurements were performed with a BAS-100B electrochemical analyzer connected a PA-1 preamplifier (Bioanalytical Systems Inc., USA). A three-electrode system, one of the resulted electrodes, platinum wire and saturated calomel electrode (SCE) were employed as the working, auxiliary, and reference electrodes, respectively, was used for all electrochemical experiments. The real geometry area of the working electrode was determined by the slope of plot of the anodic peak current of 1.0 mM $K_3[Fe(CN)_6]$ in 0.1 M KCl vs. the square root of scan rate to be 1.9×10^{-3} cm^2. All experiments were performed at room temperature (27 ± 2 °C) in 0.1 M PBS as background electrolyte. All experimental solutions were deoxygenated by bubbling highly pure nitrogen for 15 min and maintained under nitrogen atmosphere during the course of the experiment. The AC impedance experimental was carried out with a CHI660 electrochemistry workstation (CHI Co., USA) with a frequency range of 1 Hz − 10 kHz. Amperometric experiments were carried out in a stirred cell with a successive addition of 20 μL 2.0 mM $NaNO_2$ to 5.0 mL supporting solution by applying a potential step of − 950 mV to the Mb-Au-CPE.

3. Results and Discussion

3.1. Direct Electrochemistry of Mb Immobilized CPE

The cyclic voltammogram of the Mb-Au-CPE in pH 7.0 PBS exhibited a couple of stable and well-defined redox peaks at − 315 and − 378 mV at 50 mV s^{-1}, as shown in Figure 1, while no peak was observed at either CPE or Au-CPE which displayed a slow background current. Obviously, the response of Mb-Au-CPE was attributed to the redox of the electroactive center of immobilized Mb. The presence of gold colloid resulted in a slight decrease in the background current. When Mb was immobilized in CPE without the presence of gold colloid, the Mb-CPE showed the response of Mb (Fig. 1c). However, the redox peaks were asymmetric and the oxidation peak current was much smaller than its reduction peak current. The presence of colloidal gold resulted in a great increase of oxidation peak current of Mb due to the negative-charged surface of colloidal gold particles (Fig. 1d). The oxidation peak current of Mb in Au-CPE was 3.4 times larger than that in CPE. The peak-to-peak separation of Mb-Au-CPE at 50 mV s^{-1} was 62 mV, while Mb-CPE gave a value of 100 mV. Thus colloidal gold particles facilitated the electron transfer of Mb due to the

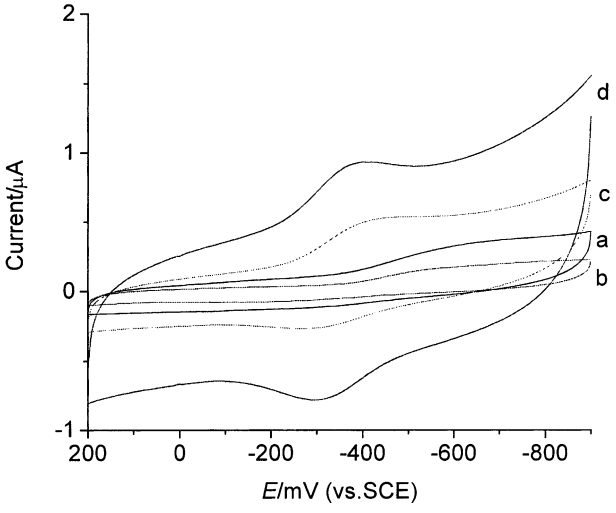

Fig. 1. Cyclic voltammograms of CPE (a), Au-CPE (b), Mb-CPE (c) and Mb-Au- CPE (d) in 0.1 M pH 7.0 PBS at 50 mV s^{-1}.

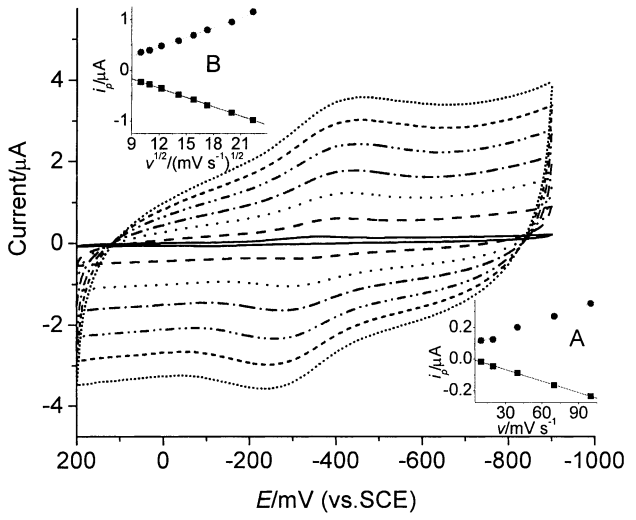

Fig. 2. Cyclic voltammograms of Mb-Au -CPE in pH 7.0 PBS at 10, 40, 120, 200, 300, 400 and 500 mV s^{-1} (from inner to outer). Inset A: Plot of peak current vs. v. Inset B: Plot of peak current vs. $v^{1/2}$.

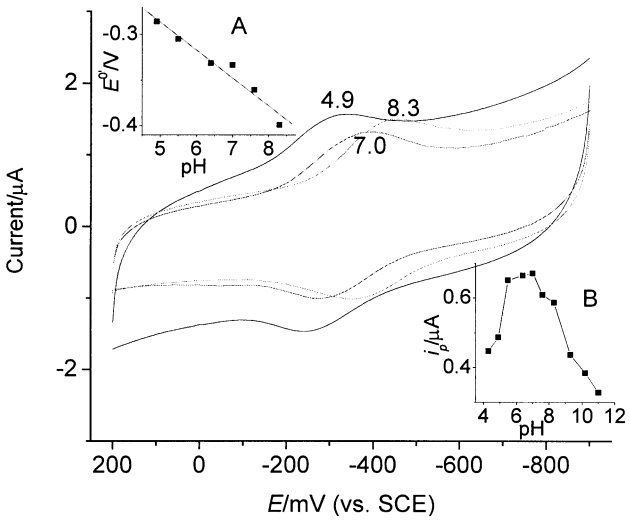

Fig. 3. Cyclic voltammograms of Mb-Au-CPE in PBS with different pHs at 50 mV s^{-1}. Inset A: Effect of pH on the formal potential. Inset B: Dependence of cathodic peak current on solution pH.

improvement of microenvironment for electron transfer of redox protein.

3.1.1. Electron Transfer Process of Mb Immobilized on Au-CPE

Figure 2 shows the CV curves of the Mb-Au-CPE at different scan rates. The voltammograms give a well-defined peak shape. With an increasing scan rate the anodic peak potential of Mb shifts to a more positive value and the cathodic peak potential shifts in a negative direction. In the scan rate range of 10 – 100 mV s^{-1}, the redox peak currents are proportional to the scan rate (inset A in Fig. 2), thus both electrode reactions are typical of the surface-controlled quasi-reversible process. The peak-to-peak separation of 19 mV at 10 mV s^{-1} indicates a rather fast electron transfer. The presence of gold nanoparticles avoids the need of promoter molecules for electron exchange between Mb and carbon sensing sites.

When the scan rate is larger than 100 mV s^{-1}, the redox peak currents are proportional to the square root of scan rate, $v^{1/2}$ (inset B in Fig. 2). According to the dependence of formal potential of immobilized Mb on solution pH (Fig. 3), the electrode process involves the participation of proton for neutralizing the excess charge in electrode reaction process. Thus, a proton gradient is produced during the electrochemical reaction at high scan rates. The involvement of the proton gradient results in an electron transfer process with diffusion-controlled behavior [34]. Considering the change in peak potential and the ratio near unity for the cathodic to anodic peak currents, the redox reactions are typical of a diffusion-controlled quasi-reversible process. The diffusion of protons is the rate-limiting step at the scan rates more than 100 mV s^{-1}.

3.1.2. Coverage of Mb Immobilized on Au-CPE

From the integration of the reduction peak of Mb immobilized on Au-CPE at scan rates less than 100 mV s^{-1}, the average surface coverage of Mb, Γ ($\Gamma = Q/nFA$ and A is 1.9×10^{-3} cm^2), is calculated to be $(3.17 \pm 0.13) \times 10^{-10}$ mol cm^{-2}. The coverage is similar to those of $(2.72 \pm 0.01) \times 10^{-10}$ mol cm^{-2} at Mb-$2C_{12}N + PVS^-$ modified electrode [35] and 2.785×10^{-10} mol cm^{-2} at Mb-Hcy/Au electrode [36], showing a monolayer coverage of Mb on gold colloid modified CPE.

3.1.3. Formal Potential of Mb Immobilized on Au-CPE

The formal potential of Mb calculated from the average of anodic and cathodic peak potentials in the scan rate range from 10 to 500 mV s^{-1} is $-(0.349 \pm 0.002)$ V which is (-0.108 ± 0.002) V (vs. NHE). This value is close to its standard potential of -0.049 V (vs. NHE) for MbFe(III) reduction to MbFe(II) [37] and the values of -0.335 V (vs. SCE) at Mb-PAM [30] and -0.362 V (vs. SCE) at Mb-AQ [17], suggesting the Mb molecules immobilized on the surface of the colloidal gold nanoparticles preserve their native structure.

3.1.4. Electron Transfer Kinetics of Mb Immobilized on Au-CPE

At scan rates less than 100 mV s^{-1}, the surface electron transfer kinetics can be analyzed using the model of Laviron [38]. The plot of cathodic peak potentials vs. the logarithm of scan rates gives a charge transfer coefficient α of 0.507. The peak-to-peak separations are 19, 45, 70, 74 and 83 mV at 10, 20, 40, 70, and 100 mV s^{-1}, respectively. Considering the α

value between 0.3 and 0.7 and the peak-to-peak separations less than 100 mV, the electron transfer rate constant k_s estimated according to the formula $k_s = mnFv/RT$ to be $(26.7 \pm 3.7)\ s^{-1}$, where m is a parameter related to the peak-to-peak separation. The large k_s value indicates a fast electron transfer rate, which is much faster than that of Mb immobilized on a DL-homocysteine self-assembled gold electrode at which the k_s value was $0.93\ s^{-1}$ [36].

3.2. Effect of Solution pH on Direct Electron Transfer of Immobilized Mb

In most cases, protein redox behavior is often significantly dependent on the solution pH. Cyclic voltammograms of Mb-Au-CPE in PBS also showed a strong dependence on solution pH (Fig. 3). All changes in CV peak potentials and currents with pH were reversible in the pH range of 4.9 to 8.3, that is, the same CV could be obtained if the electrode was transferred from a solution with a different pH value to its original solution. An increase in solution pH caused a negative shift in both cathodic and anodic peak potentials. Plot of the formal potential versus pH produced a line with the slope of $-30.6 \pm 3.4\ mV\ pH^{-1}$ (inset A in Fig. 3), half of the theoretical value of $-59\ mV\ pH^{-1}$ for a reversible proton-coupled single electron transfer at 25 °C as observed at Mb-$2C_{12}N + PVS^-$ modified electrode [35]. The participation of proton in the electron transfer process was to neutralize the excess charge that accumulated at the interface upon electrochemical reduction.

Inset B in Figure 3 shows the relationship between the peak currents of the Mb immobilized on Au-CPE and the solution pH. It is clearly observed that an optimal pH range occurs between 5.0 and 7.0 with a maximum peak current at pH 7.0, the isoelectric point of Mb [39]. The same result was also observed for Mb at an indium oxide electrode [5], indicating the entrapped process does not alter the optimal pH value for electron transfer of immobilized Mb.

3.3. Impedance Characterization of Mb-Au-CPE

The effect of colloidal gold nanoparticles on the impedance of carbon paste electrode was investigated using AC impedance spectroscopy. An equivalent circuit was utilized to model the impedance data, thus enabling the extraction of electrical parameters, such as resistance, from the impedance spectra [40, 41].

Figure 4 shows the AC impedance spectra of the CPE (a), Au-CPE (b), Mb-CPE (c), and Mb-Au-CPE (d), respectively, obtained in 0.1 M pH 7.0 PBS. It is clearly observed

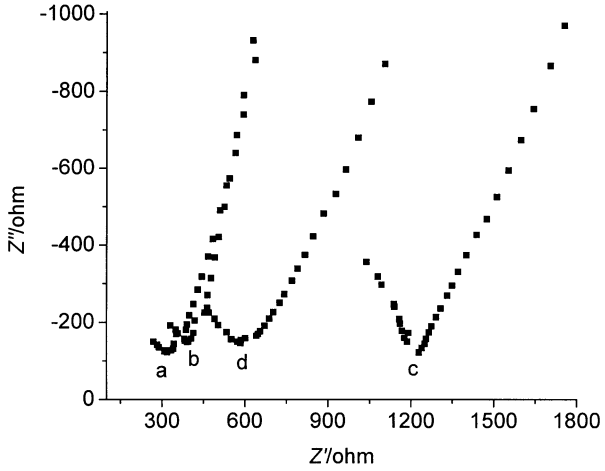

Fig. 4. AC impedigrams of CPE (a), Au-CPE (b), Mb-CPE (c) and Mb-Au-CPE (d).

that the polarization impedance, the resistance of electron transfer in electrode reaction, increases slightly upon addition of colloidal gold to carbon paste (curves a and b in Fig. 4). An obvious increase in polarization impedance is observable upon addition of Mb to carbon paste (curves a and c in Fig. 4). The colloidal gold, however, can decrease greatly the polarization impedance of Mb-CPE (curves c and d in Fig. 4). The increase in polarization impedance upon addition of gold colloid is due to the ratio decreasing of carbon sensing sites in the paste. The results of data analysis of impedigrams are given in Table 1.

3.4. Electrocatalysis of Mb Immobilized in Au-CPE to Reduction of H_2O_2

Upon addition of H_2O_2 to PBS, the shape of cyclic voltammogram of Mb-Au-CPE for the direct electron transfer of Mb changed dramatically with an increase of reduction current (Fig. 5), while no obvious change was observed at CPE and Au-CPE. The increase in reduction peak and the decrease in oxidation peak current of Mb at Mb-Au-CPE displayed an obvious electrocatalytic behavior of immobilized Mb to the reduction of H_2O_2. Furthermore, the reduction peak current increased with an increasing H_2O_2 concentration. This electrocatalytic response to the reduction of H_2O_2 was also observed at Mb-CPE. The electrocatalytic current, however, is about 62.9% of that at Mb-Au-CPE at the H_2O_2 concentration of 20 μM. The electrocatalytic process can be expressed as follows [6]:

$$H_2O_2 + 2MbHFe(II) \rightarrow 2MbFe(III) + 2H_2O \quad (1)$$

Table 1. Data analysis of the impedance for different electrodes on three measurements

Electrodes	a CPE	b Au-CPE	c Mb-CPE	d Mb-Au-CPEd
Polarization impedance (Ω)	366 ± 17	471 ± 21	1207 ± 44	588 ± 23

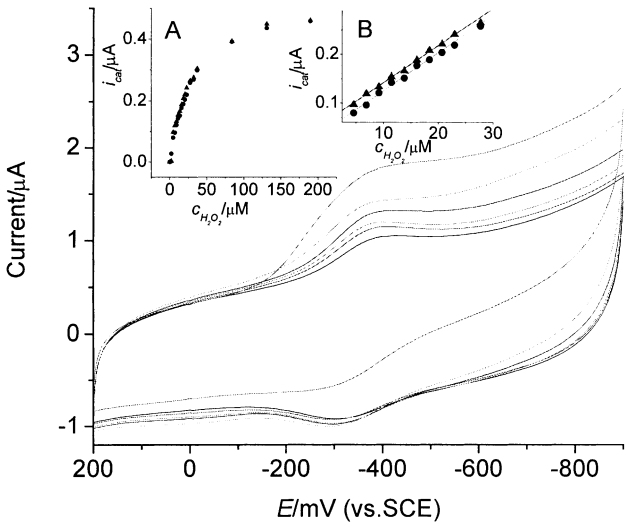

Fig. 5. Cyclic voltammograms of Mb-Au-CPE in pH 7.0 PBS containing 0, 6.9, 13.8, 18.4, 84.1 and 760 μM H_2O_2 at 50 mV s^{-1}. Inset A: Plots of electrocatalytic currents at −0.380 (●) and −0.425 V (▲) vs. H_2O_2 concentration. Inset B: Linear calibration plots.

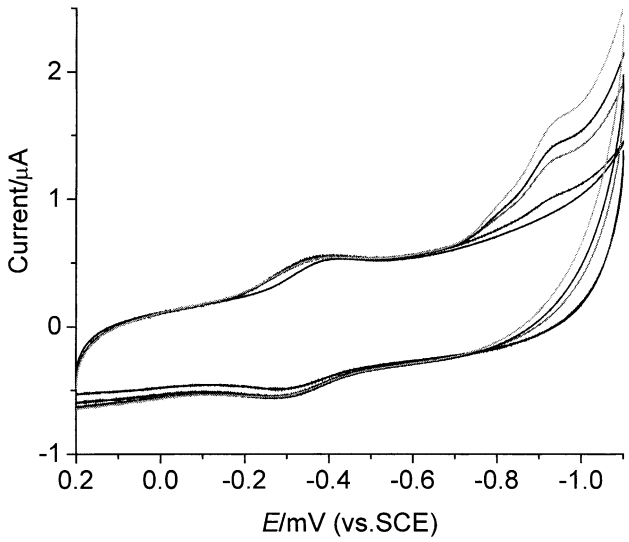

Fig. 6. Cyclic voltammograms of Mb-Au-CPE in pH 7.0 PBS containing 0, 12, 32, 56 and 80 μM $NaNO_2$ at 50 mV s^{-1} (from bottom to top).

In the presence of H_2O_2, MbHFe(II) was efficiently converted to its oxidized form, MbFe(III). Consequently, MbFe(III) was reduced at the electrode surface by the direct electron transfer.

With increasing H_2O_2 concentration the current response for MbFe(III) reduction increased (Fig. 5). The insets in Figure 5 indicate that the electrocatalytic current increases with successive addition of H_2O_2. The calibration range of H_2O_2 is from 4.6 μM to 2.0 mM with a linear relation from 4.6 μM to 28 μM ($R = 0.9973$ at −0.380 V and 0.9977 at −0.425 V). The variation coefficient is 4.7% for six successive assays of 10 μM H_2O_2 at −0.380 V.

When the concentration of H_2O_2 was higher than 28 μM, a platform was observed, showing a characteristic of the Michaelis-Menten kinetic mechanism. The apparent Michaelis-Menten constant (K_M^{app}), a reflection of both the enzymatic affinity and the ratio of microscopic kinetic constants, can be obtained from the electrochemical version of the Linweaver-Burk equation [42]. The K_M^{app} value for Mb-Au-CPE was found to be 0.65 ± 0.02 mM at both −0.380 and −0.425 V, which was lower than those of 2.28 mM at cyt.c/Au-CPE [24], 3.69 mM at HRP-Au-CPE [25], 5.5 mM for membrane-entrapped HRP [33] and 2.3 mM for HRP/Au colloid self-assemble monolayer electrode [43]. Thus, Mb molecules entrapped in the mixture of Au colloid and carbon paste is of a higher affinity to H_2O_2.

3.5. Electrocatalysis of Mb Immobilized in Au-CPE to Reduction of Nitrite

When NO_2^- was added into PBS, the cyclic voltammogram of Mb-Au-CPE displayed a new reduction peak at about −0.9 V, while the pair of redox peaks for MbFe(III)/Fe(II) remained intact (Fig. 6) and no obvious peak was observed at either Au-CPE or CPE, indicating a promoting action of immobilized Mb to the electrochemical reduction of nitrite. This phenomenon was similar to the direct reduction of nitrite at Mb-DDAB film [14, 44] and at Mb-PAM film modified PG electrodes [30]. Although the immobilized Mb in CPE without the presence of colloidal gold also showed an electrocatalytic response to the reduction of nitrite, the catalytic current at −840 mV was only 42.1% of that at Mb-Au-CPE at the nitrite concentration of 32 μM.

Figure 7 shows a typical hydrodynamic current-time response of Mb-Au-CPE at −950 mV upon successive addition of $NaNO_2$ to 0.1 M pH 7.0 PBS. Upon the addition

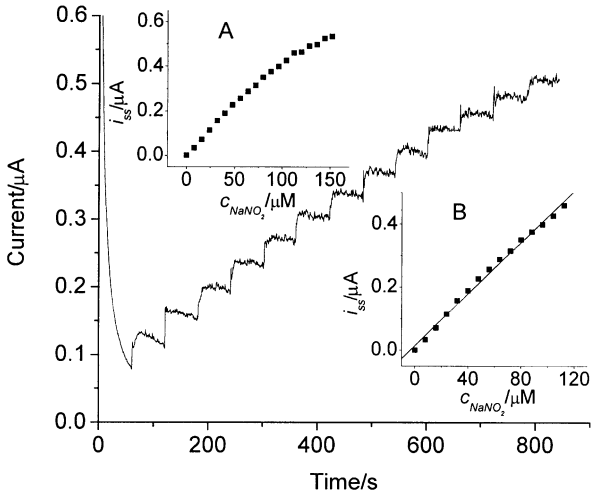

Fig. 7. Amperometric response of the Mb-Au-CPE at −950 mV upon successive additions of 20 μL 2 mM $NaNO_2$ to 5.0 mL pH 7.0 PBS. Inset A: Plot of steady-state current vs. NO_2^- concentration. Inset B: Linear calibration plot.

the electrode achieved 93% of steady-state current within 5 s, indicating a fast amperometric response to $NaNO_2$ reduction. The sensor shows an increasing amperometric response to $NaNO_2$ from 8.0 to 152 μM (inset A in Fig. 7) with a linear range from 8.0 to 112 μM ($r = 0.997$ for n value of 15, shown as inset B in Fig. 7). The detection limit is 0.7 μM at 3 σ. The sensitivity was much better than that reported for the detection limit of 0.1 mM NO_2^- [30].

3.6. Stability and Renewal of the Sensor

After Mb-Au-CPE was stored in PBS at 4 °C for 20 days or successively used for 150 times, no obvious decrease in the amperometric response was observed. After a 28-day storage period, the sensor retained 90% of its initial current response. Thus colloidal gold mixed in carbon paste was very efficient for retaining the activity of Mb and preventing it from leaking out of the sensor.

After the sensor was stored for 40 days, the response of the sensor decreased irreversibly due to the Mb leaking out from the surface of sensor. The surface could be renewed by a gently rubbing on a fine paper. The current response of the renewed surface was examined at a H_2O_2 concentration of 10 μM. The relative standard deviation was 4.6% for six successive renewals. Thus the method was rapid, easy and, more importantly, reproducible to remove surface Mb film.

4. Acknowledgements

The authors gratefully acknowledge the financial support of the National Natural Science Foundation of China (29975013 and 29835110), the Doctoral Program for Higher Education from the Education Ministry of China (200028403), the Natural Science Foundation of Jiangsu (BS2001063) and the Opening Laboratory of Electroanalytical Chemistry, Changchun Institute of Applied Chemistry.

5. References

[1] E. D. Bowden, F. M. Hawkridge, H. N. Blount, Bioelectrochemistry, in Coprehensive Treatise of Electrochemistry (Eds: S. Srinivasan, Y. A. Chizmadzhev, J. O.'M. Bockris, B. E. Conway, E. Yeager), Plenum Press, New York **1985**, p. 297.
[2] F. Scheller, M. Janchen, G. Etzold, H.Will, *Bioelectrochem. Bioenerg.* **1974**, *1*, 478.
[3] J. F. Stargardt, F. M. Hawkridge, H. L. Landrum, *Anal. Chem.* **1978**, *50*, 930.
[4] E. D. Bowden, F. M. Hawkridge, H. N. Blount, *Bioelectrochem. Bioenerg.* **1980**, *7*, 447.
[5] I. Taniguchi, K. Watanabe, M. Tominaga, F. M. Hawkridge, *J. Electroanal. Chem.* **1992**, *333*, 331.
[6] S. Dong, Q. Chi, Chin. *J. Chem.* **1993**, *11*, 12.
[7] B. C. King, F. M. Hawkridge, *J. Electroanal. Chem.* **1987**, *237*, 81.
[8] J. F. Rusling, A-E. F. Nassar, *J. Am. Chem. Soc.* **1993**, *115*, 11891.
[9] A-E. F. Nassar, W. S. Willis, J. F. Rusling, *Anal. Chem.* **1995**, *67*, 2386.
[10] K. Toko, N. Nakashima, S. Iryama, K. Yamajuji, T. Kunitake, *Chem. Lett.* **1986**, 1375.
[11] Y. Okahata, G. Enna, K. Taguchi, T. Seki, *J. Am. Chem. Soc.* **1985**, *107*, 5300.
[12] Y. Okahata, G. Enna, *J. Phys. Chem.* **1988**, *92*, 4546.
[13] J. F. Rusling, *Acc. Chem. Res.* **1998**, *31*, 363.
[14] D. Mimica, J. H. Zagal, F. Bedioui, *J. Electroanal. Chem.* **2001**, *497*, 106.
[15] Z. Salamon, G. Tollin, *Bioelectroanal. Bioenerg.* **1991**, *25*, 447.
[16] H. Ohno, Y. Nakai, *Polymer. J.* **1999**, *31*, 1145.
[17] N. Hu, J. F. Rusling, *Langmuir* **1997**, *13*, 4119.
[18] T. Huang, A. Warsinke, T. Kuwana, F. W. Scheller, *Anal. Chem.* **1998**, *70*, 991.
[19] T. Ikeda, H. Hamada, K. Miki, M. Senda, *Agric. Biol. Chem.* **1985**, *49*, 541.
[20] J. Kulys, Biosens. *Bioelectron.* **1999**, *14*, 473.
[21] J. Wang, A. Ciszewski, N. Naser, *Electroanalysis* **1992**, *4*, 777.
[22] C. Petit, A. Gonzalez-Cortes, J – M. Kauffmann, *Talanta* **1995**, *42*, 1783.
[23] K. R. Brown, A. P. Fox, M. J. Natan, *J. Am. Chem. Soc.* **1996**, *118*, 1154.
[24] H. X. Ju, S. Q. Liu, B. Ge, F. Lisdat, F. W. Scheller, *Electroanalysis* **2002**, *14*, 141.
[25] S. Q. Liu, H. X. Ju, *Anal. Biochem.* **2002**, *307*, 110.
[26] J. Davis, R. G. Campton, *Anal. Chim. Acta* **2000**, *404*, 241.
[27] J. Wang, Y. Lin, L. Chen, *Analyst* **1993**, *118*, 277.
[28] T. J. O'Shea, D. Leech, M. R. Smyth, J. G. Vos, *Talanta* **1992**, *39*, 443.
[29] I. T. Bae, R. L. Barbour, D. A. Scherson, *Anal. Chem.* **1997**, *69*, 249.
[30] L. Shen, R. Huang, N. Hu, *Talanta* **2002**, *56*, 1131.
[31] M. G. Garguilo, N. Huynh, A. Proctor, A. C. Michael, *Anal. Chem.* **1993**, *65*, 523.
[32] G. Jöensson – Pettersson, *Electroanalysis* **1991**, *3*, 741.
[33] T. Ferri, A. Poscia, R. Santucci, *Bioelectrochem. Bioenerg.* **1998**, *45*, 221.
[34] A. P. Brown, F. C. Anson, *J. Electroanal. Chem.* **1978**, *92*, 133.
[35] Y. Hu, N. Hu, Y. Zeng, *Microchem. J.* **2000**, *65*, 147.
[36] H. M. Zhang, N. Q. Li, *Bioelectrochem.* **2000**, *53*, 97.
[37] P. A. Loach, Handbook of Biochemistry Selected Data for Molecular Biology, 2nd ed. (Ed: H. A. Sober), CRC Press, Cleveland, OH. **1970**, pp. J33 – J40.
[38] E. Laviron, *J. Electroanal. Chem.* **1979**, *101*, 19.
[39] A. J. Bard, L. R. Faulkner, Electrochemical Methods, Wiley, Now York **1980.**
[40] M. L. Shi, Z. Y. Chen, J. Sun, *Cement and Concrete Research* **1999**, *29*,1111.
[41] A. L. Lehninger, Biochemistry: The Molecular Basic of Cell Structure and Function (2nd ed.), Worth Publisher, **1975**, ch. 7.
[42] R. A. Kamin, G. S. Willson, *Anal. Chem.* **1980**, *52*, 1198.
[43] Y. Xiao, H. X. Ju, H. Y. Chen, *Anal. Biochem.* **2000**, *278*, 22.
[44] R. Lin, M. Bayachou, J. Greaves, P. J. Farmer, *J. Am. Chem. Soc.* **1997**, *119*, 12689.

